AIAA 81-4159

Assessment of Propeller Influence on Lateral-Directional Stability of Multiengine Aircraft

R. S. van Rooyen* and M. E. Eshelby†
Cranfield Institute of Technology, Cranfield, Bedford, United Kingdom

Using a twin-engine turboprop aircraft, flight measurements were made to supplement the very limited data on the effects of propellers on the individual lateral static and dynamic stability derivatives. It is found that the propeller slipstream significantly affects the wing contribution to the derivative l_v. A significant reduction in recovery time from the spiral mode instability in low-speed, high-power conditions is consequently found. Propeller disk contribution to the overall damping in yaw derivative n_r is also found to be significant. Propeller contributions to y_v and n_v, due to the known "fin" effect, are found to be small for the test aircraft. Existing expressions to calculate propeller influence on l_v, n_v, and y_v are shown to be adequate, while an expression to calculate the propeller contribution to n_r, which appears not to have been analyzed before, is presented.

Nomenclature

a_y = lateral acceleration
b = wing span
C_{Di} = drag coefficient of slipstream-immersed wing area $= D_i/q_\infty S$
C_N = yawing moment coefficient $= N/\rho n^2 D^5$
C_T = thrust coefficient $= T/\rho n^2 D^4$
C_Y = sideforce coefficient $= Y/\rho n^2 D^4$
D = propeller diameter
D_i = drag of a slipstream-immersed wing area
I_x, I_z = moments of inertia with relation to X and Z body axes
I_{xz} = product of inertia with relation to X and Z body axes
i_p = incidence of propeller shaft with relation to X body axes
J = advance ratio $= V/nD$
L = rolling moment about X body axis
l_p = $\partial L/\partial p/(\frac{1}{4}\rho VSb^2)$
l_r = $\partial L/\partial r/(\frac{1}{4}\rho VSb^2)$
l_v = $\partial L/\partial v/(\frac{1}{2}\rho VSb)$
l_ξ = $\partial L/\partial \xi/(\frac{1}{2}\rho V^2 Sb)$
l_ζ = $\partial L/\partial \zeta/(\frac{1}{2}\rho V^2 Sb)$
m = aircraft mass
N = yawing moment about Z body axis
N_p = number of propellers
n = propeller rotational velocity, rps
n_p = $\partial N/\partial p/(\frac{1}{4}\rho VSb^2)$
n_r = $\partial N/\partial r/(\frac{1}{4}\rho VSb^2)$
n_v = $\partial N/\partial v/(\frac{1}{2}\rho VSb)$
n_ξ = $\partial N/\partial \xi/(\frac{1}{2}\rho V^2 Sb)$
n_ζ = $\partial N/\partial \zeta/(\frac{1}{2}\rho V^2 Sb)$
q_∞ = freestream dynamic pressure $= \frac{1}{2}\rho V^2$
$\Delta\bar{q}$ = mean slipstream dynamic pressure relative to q_∞
r = blade radius, rate of yaw
S = wing area
T = thrust force per propeller
T_c' = total thrust coefficient $= N_p T/q_\infty S$
V = forward velocity
v = slipstream velocity relative to Y
X, Y, Z = orthogonal set of aircraft body axes
x = nondimensional blade radius $= 2r/D$
Y = side force
y_T = lateral displacement of propeller shaft
y_v = $\partial Y/\partial V/(\rho VS)$
y_ξ = $\partial Y/\partial \xi/(\rho V^2 S)$
y_ζ = $\partial Y/\partial \zeta/(\rho V^2 S)$
z_T = vertical displacement of propeller disk center
$(\dot{})$ = $\mathrm{d}(\ )/\mathrm{d}t$
α = incidence of X body axis
β = sideslip angle
Δ = incremental value
ρ = air density
ϕ = bank angle
θ = blade azimuth angle
ψ = yaw angle
σ_p = slipstream sidewash angle
ϵ_p = slipstream downwash angle
ξ_m = mean aileron angle $= \frac{1}{2}(\xi_p + \xi_s)$
ζ = rudder angle
Θ = pitch angle of X body axis
τ = $2m/\rho SV$
μ = $2m/\rho Sb$

Subscripts

ΔC_D = wing drag differential due to r
ΔC_T = propeller thrust differential due to r
fin = propeller "fin" effect
i = inboard propeller
na = engine nacelle
o = outboard propeller
p = rate of roll, port, propeller
$\Delta\bar{q}$ = slipstream dynamic pressure influence
r = rate of yaw, radial inflow velocity
s = starboard
v = vane measurement
α = differentiation with relation to α
ϵ_p = slipstream downwash influence
σ_p = slipstream sidewash influence
0.75 = 0.75 blade radius

Received Feb. 26, 1980; revision received July 7, 1980.

*Graduate Student, College of Aeronautics (currently Senior Research Officer, National Institute for Aeronautics and Systems Technology, South Africa).

†Lecturer in Flight Mechanics, College of Aeronautics. Member AIAA.

Introduction

PROPELLER influence on aircraft stability was recognized as early as 1909, and the importance of this influence has increased since the advent of modern turboprop aircraft due to the high engine output and propeller solidities involved. Apart from the fact that the propeller is still a propulsor of considerable importance, renewed emphasis is

placed on relevant propeller research with the development now in progress of Mach 0.8 cruise propfans for use in aircraft in the late 1980s which will offer considerably lower energy consumption than turbofans. The total propeller contribution to stability increases with the number of engines on a particular aircraft type, and therefore propeller influence may be of particular importance to a multiengine aircraft.

Propeller influence may be due either to forces and moments experienced by the propeller when operating in an asymmetrical flowfield, or to the interference between the propeller slipstream and other parts of the aircraft's structure. In this study, attention will be paid to: 1) Effects on stability due to the propeller blade forces and 2) Propeller slipstream influence on the wing contribution to stability.

The significance of stability contributions resulting from propeller blade forces acting in the plane of the disk increases with speed, while that of forces normal to the disk plane decreases with speed. The significance of propeller slipstream contributions increases with decrease in speed and increase in power since the dynamic pressure in the slipstream increases relative to the freestream dynamic pressure.

Although ample wind-tunnel results for isolated propellers with asymmetric inflow are available, there does not appear to be any flight data and, for that matter, only limited wind-tunnel data[1-3] concerned with propeller contributions to the individual lateral stability derivatives for the case of the installed propeller. Such data are necessary to determine the merit of the existing predictions of propeller static stability derivatives, since these expressions have in fact been derived for uninstalled (or isolated) propellers. Very limited data[3] concerned with propeller contributions to the rotary derivatives are available.

The object of this study is to provide flight data to supplement the limited experimental data about the influence of propellers on individual static and dynamic lateral stability derivatives of multiengine aircraft to allow an assessment to be made of the significance of these effects. Flight data are also presented in relation to existing analytical predictions and where expressions to estimate significant propeller effects on certain derivatives are not available, formulas are presented. Other possible propeller effects on aircraft handling such as asymmetric stall, propeller yawing moment at high aircraft incidence, and propeller-induced sideslip are not discussed in this paper.

Experimental Procedure

To observe propeller influence on stability, a method was employed by which the test aircraft's stability was measured at different engine power settings. The trends of variation in the individual stability derivatives with variations in power were then analyzed to assess the significance of the propeller contributions to these derivatives. Possible significant propeller influence was explored using 50 and 20 deg flap selections at the low-speed end, and a clean configuration at the high-speed end. The "maximum-likelihood" parameter estimation technique was used to extract derivatives from the recorded time histories of control inputs and aircraft responses for every maneuver executed at each power condition. To attribute variations in stability to power effects only, the test aircraft was flown at constant incidence by means of an incidence vane angle display. This was necessary since variations in incidence (and therefore in stability) would have occurred with large variations in power if a technique had been followed by which the speed was kept constant for different power settings. This is due to the variation in lift increments of the slipstream-immersed wing areas, and would be particularly apparent at low-speed conditions with the flaps selected.

The control inputs employed to perturb the aircraft from its trimmed condition in order to extract a full set of lateral stability and control derivatives were an aileron doublet and a step-rudder input initiated at the same time. To isolate propeller side force at the high-speed end, dutch rolls were initiated and sustained by rudder pedaling with the ailerons held neutral. Control deflections and sideslip and incidence vane angles were measured by rotary inductive pickoffs; roll rate, yaw rate, and lateral acceleration by rate gyroscopes and an accelerometer in a c.g. pack. Outputs were recorded on magnetic tape; data were obtained at 20 samples/s. Air speed, pressure altitude, outside air temperature, fuel flow, fuel state, and propeller blade pitch were measured and noted manually.

The test aircraft was an HP 137 turboprop with two three-bladed Hamilton Standard 23LF propellers of 2.591 m diam running at constant 1783 rpm. The variable pitch range in flight was 7-32 deg. For full power and maximum continuous power, the pitch is adjusted automatically to maintain constant shaft power and adjusted manually for other power values.

The aircraft mass, c.g. position, and rolling moment of inertia were obtained experimentally.[4] The manufacturer's estimates of product of inertia and yawing moment of inertia were used.

Equations of Motion

It is assumed that the stability derivatives may be written as the sum of the basic power-off values and the power-on increments:

$$\lambda_{\text{power}} = \lambda_{\substack{\text{prop}\\ \text{off}}} + \Delta(\lambda)_{\text{power}} \tag{1}$$

The general power-on, nondimensional, lateral-directional, small perturbation equations of motion referred to a system of body axes are given by:

$$\dot{\beta} = p\sin\alpha - r\cos\alpha + (2/\tau)\beta y_{v(\text{power})} + (g/V)\phi\cos\Theta + (2/\tau)y_\zeta\zeta \tag{2}$$

$$\dot{p} - I_{xz}/I_x\dot{r} = (mb^2/I_x\tau)\{\tfrac{1}{2}pl_{p(\text{power})} + \tfrac{1}{2}rl_{r(\text{power})} + (\mu/\tau)\beta l_{v(\text{power})} + (\mu/\tau)\xi l_\xi + (\mu/\tau)\zeta l_\zeta\} \tag{3}$$

$$\dot{r} - I_{xz}/I_z\dot{p} = (mb^2/I_z\tau)\{\tfrac{1}{2}pn_{p(\text{power})} + \tfrac{1}{2}rn_{r\,(\text{power})} + (\mu/\tau)\beta n_{v(\text{power})} + (\mu/\tau)\xi n_\xi + (\mu/\tau)\zeta n_\zeta\} \tag{4}$$

$$\dot{\phi} = p \tag{5}$$

It has been assumed that the side-force derivatives y_p,y_r, and y_ξ are insignificant, and the second-order term $\psi\sin\Theta$ in Eq. (2) has been neglected. The linearized equations of motion can be, after rearrangement, written in the form $\dot{x} = Ax + Bu$ which, together with a set of equations describing the output responses, represents a system which can be described by:

$$\dot{x} = Ax + Bu \tag{6}$$

$$y = Cx + Du \tag{7}$$

$$z = y + n \tag{8}$$

where

$x^T = [p, r, \beta, \phi]$, the state vector

$u^T = [\xi_m, \zeta]$, the input vector

$y^T = [p, r, \beta_v, a_y]$, the output vector

z = the measured output vector

n = vector containing the measured white noise

A computer program[5] employing the maximum-likelihood parameter estimation technique was used to identify the stability and control derivatives contained in the matrices A,

B, *C*, and *D* of the system described by Eqs. (6-8), as well as the error bounds on the derivatives.

Discussion of Results

In NASA TN D-6946[6] most of the possible propeller effects are discussed and methods given to estimate these contributions to stability. Only the basic equations will be given in this paper, except in cases where an analysis has not been conducted. Equations are presented for the case of a four-engine aircraft of conventional geometry. Propeller effects due to phase angle lag of the propeller force and moment system relative to blade azimuth are of secondary importance and have been neglected.

The trends of the data for the 50 and 20 deg flap configurations were found to be similar, and only the data for the 50 deg flap case is presented here as typical of the data obtained at low-speed conditions.

Propeller Side Force due to Sideslip

Propeller effects on y_v consist of the propeller side-force contribution due to the "fin" effect, a change in nacelle contribution to y_v due to the increased dynamic pressure in the slipstream, and a propeller side-force-induced sidewash of the slipstream which effects the nacelle contribution:

$$\Delta(y_v)_{\text{power}} = N_p[\Delta(y_v)_{\text{fin}} + \Delta(y_v)_{na(\Delta\bar{q})} + \Delta(y_v)_{na(\sigma_p)}] \quad (9)$$

where

N_p = number of propellers

$$(y_v)_{\text{fin}} = \frac{D^2 C_Y}{SJ^2\beta} \quad (10)$$

$$\Delta(y_v)_{na(\Delta\bar{q})} = [(y_v)_{na}]_{\substack{\text{prop}\\\text{off}}} \frac{\Delta\bar{q}}{q_\infty} \quad (11)$$

$$(y_v)_{na(\sigma_p)} = -[(y_v)_{na}]_{\substack{\text{prop}\\\text{off}}} \frac{\partial\sigma_p}{\partial\beta}\left(1+\frac{\Delta\bar{q}}{q_\infty}\right) \quad (12)$$

It can be shown that $\Delta(y_v)_{\text{fin}}$ [Eq. (10)] will have maximum significance at maximum speed, while the slipstream-dependent terms $\Delta(y_v)_{na(\Delta\bar{q})}$ and $\Delta(y_v)_{na(\sigma_p)}$ will have maximum values at low-speed, full-power conditions. In a high-speed flight test $\Delta(y_v)_{\text{fin}}$ was isolated by extracting the y_v derivative from the recorded responses of sustained dutch rolls at 200 KIAS for the cases of 1) both engines running and 2) port engine shut down and propeller feathered. In Fig. 1 it can be seen that the fit between measured and calculated responses is good, and the resulting small error bounds on the extracted y_v derivative allowed a conclusion to be made about the incremental change in the total $\Delta(y_v)_{\text{fin}}$ contribution due to the shutting down of one engine. Note that the change in y_v can be attributed to $\Delta(y_v)_{\text{fin}}$ only, since it can be shown that $\Delta(y_v)_{na(\Delta\bar{q})}$ and $\Delta(y_v)_{na(\sigma_p)}$ are negligible in this condition. The feathered propeller contribution to y_v was assumed to be negligible.

The results shown in Table 1 indicate that the experimentally determined mean value of $\Delta(y_v)_{\text{fin}}$ is less than half the theoretically predicted values, but that the maximum difference between cases 1 and 2 is -0.02, which is of the order of the predicted values for $\Delta(y_v)_{\text{fin}}$, calculated by a computer simulation program of the propeller operating at asymmetric inflow conditions,[4] and a currently used expression[7] for estimating propeller side force. On the face of these limited results, it seems that the propeller "fin" effect is less than predicted, but that the existing prediction gives an

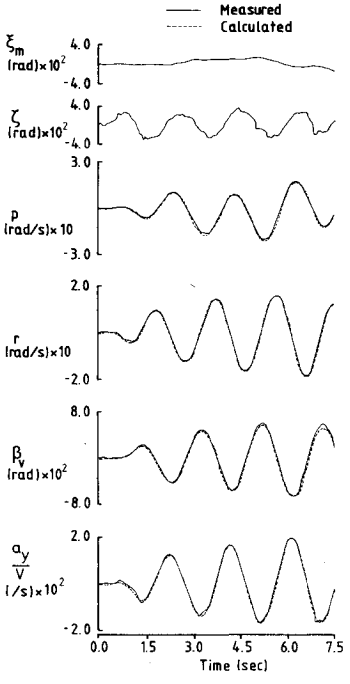

Fig. 1 Control input and response (clean configuration, 200 KIAS).

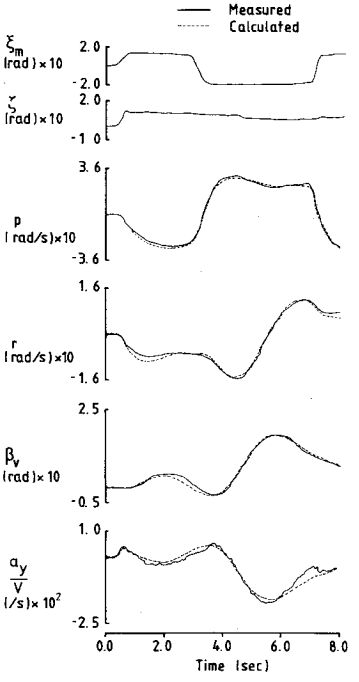

Fig. 2 Control input and response (50 deg flap, $T_c' = 0.066$).

Table 1 $\Delta(y_v)_{\text{fin}}$ at 200 KIAS

Both propellers running (case 1) y_v	Port propeller feathered (case 2) y_v	Mean difference $\Delta(y_v)_{\text{fin}}$	Propeller simulation program $\Delta(y_v)_{\text{fin}}$	De Young[7] $\Delta(y_v)_{\text{fin}}$
-0.574 ± 0.004	-0.573 ± 0.004			
-0.562 ± 0.01	-0.554 ± 0.004	~ -0.01	-0.025	-0.019
-0.568 ± 0.004	-0.557 ± 0.007			

upper boundary to this contribution. It appears from the literature that no previous attempt has been made to isolate the propeller fin effect by flight testing.

The effect of large power variation at low speed with 50 deg of flap on y_v, as extracted from the recorded aircraft responses to combined aileron-rudder control inputs (Fig. 2), is reflected in Fig. 3a. (The fit between measured and calculated responses shown in Fig. 2 is typical of the results obtained in the low-speed region with flaps selected.) The $N_p[\Delta(y_v)_{na(\Delta\bar{q})}+\Delta(y_v)_{na(\sigma_p)}]$ contribution as estimated from Eqs. (11) and (12) is shown to be only 2% of the overall y_v derivative, with small variation in thrust coefficient T_c'. The invariance of the term $N_p\Delta(y_v)_{\text{fin}}$ as calculated by the propeller simulation program for the same flight conditions is also shown. In general, the flight test results for y_v confirm these predicted trends of practically constant y_v with large variations in power. In Fig. 3a full-scale wind-tunnel results of the y_v derivative of a twin-engine light aircraft[1] are shown to be similarly invariant with power. Thus, although the propeller contribution $\Delta(y_v)_{\text{fin}}$ is significant [6% of the overall y_v for the test aircraft at these conditions (Fig. 3a)], it may be concluded that the slipstream and propeller sidewash effects on the nacelles over the range of possible thrust coefficients are of the small order of magnitude predicted by Eqs. (11) and (12).

Propeller Yawing Moment due to Sideslip

Propeller effects on n_v are due to the yawing moments produced by the propeller side-force contributions, and are written in similar form to Eq. (9):

$$\Delta(n_v)_{\text{power}}=2\sum_{l=i;o}[\Delta(n_v)_{\text{fin},l}+\Delta(n_v)_{na(\Delta q),l}+\Delta(n_v)_{na(\sigma_p),l}] \tag{13}$$

where

$$\Delta(n_v)_{\text{fin},l}=(2/b)x_{p,l}\Delta(y_v)_{\text{fin}} \tag{14}$$

$$\Delta(n_v)_{na(\Delta q),l}=(2/b)x_{n,l}\Delta(y_v)_{na(\Delta\bar{q})} \tag{15}$$

$$\Delta(n_v)_{na(\sigma_p),l}=(2/b)x_{n,l}\Delta(y_v)_{na(\sigma_p)} \tag{16}$$

where i and o refer to the inboard and outboard propeller pair, respectively, of a typical four-engine aircraft, x_p is the distance of the disk centers of a propeller pair from the origin of the X-body axis, and x_n the distance of the centers of pressure of a nacelle pair from the same origin.

Variation of $\Delta(n_v)_{\text{power}}$ with T_c' in the low-speed condition will, naturally, be similar to the variation of $\Delta(y_v)_{\text{power}}$. The destabilizing propeller contribution $2\Delta(n_v)_{\text{fin}}$ calculated using the propeller simulation program represents 4% of the overall n_v value for the test aircraft at these conditions (Fig. 3b), while the estimated slipstream contribution $2[\Delta(n_v)_{na(\Delta\bar{q})}+\Delta(n_v)_{na(\sigma_p)}]$, which should have a maximum value at the low-speed, full-power condition, is found to be negligible in the case of the test aircraft. Note that lateral displacement of the centers of pressure of the slipstream-immersed wing areas in sideslip will result in a lateral shift in wing drag which will, in principal, contribute to n_v. However, calculations have shown that this contribution is negligibly small.

The fact that $2[\Delta(n_v)_{na(\Delta q)}+\Delta(n_v)_{na(\sigma_p)}]$ is of small magnitude as estimated for the test aircraft is, in general, confirmed by the data for the overall n_v values extracted from the recorded control inputs and aircraft responses (Fig. 3b) since n_v shows little effect despite the large slipstream velocity (or thrust) variations. In Fig. 3b full-scale wind-tunnel results of n_v for the light twin-engine aircraft of Ref. 1 are also shown to be practically constant with large variations in thrust.

The importance of the destabilizing contribution $\Delta(n_v)_{\text{fin}}$ increases with increasing speed. It has been shown that existing theory estimates an upper bound on $\Delta(y_v)_{\text{fin}}$ and, since $\Delta(n_v)_{\text{fin}}$ is directly proportional to this contribution, an upper bound is thus also predicted on $\Delta(n_v)_{\text{fin}}$. The estimated value of $\Delta(y_v)_{\text{fin}}$ at 200 KIAS in the case of the test aircraft is -0.025, giving an upper boundary of -0.013 on $2\Delta(n_v)_{\text{fin}}$, which represents 9% of a propeller-off wind-tunnel scale model value for n_v at the same C_L.

Propeller Rolling Moment due to Sideslip

Propeller effects on l_v consist of a rolling moment due to the propeller side force, and a rolling moment due to the lateral displacement of the centers of pressure of the slip-

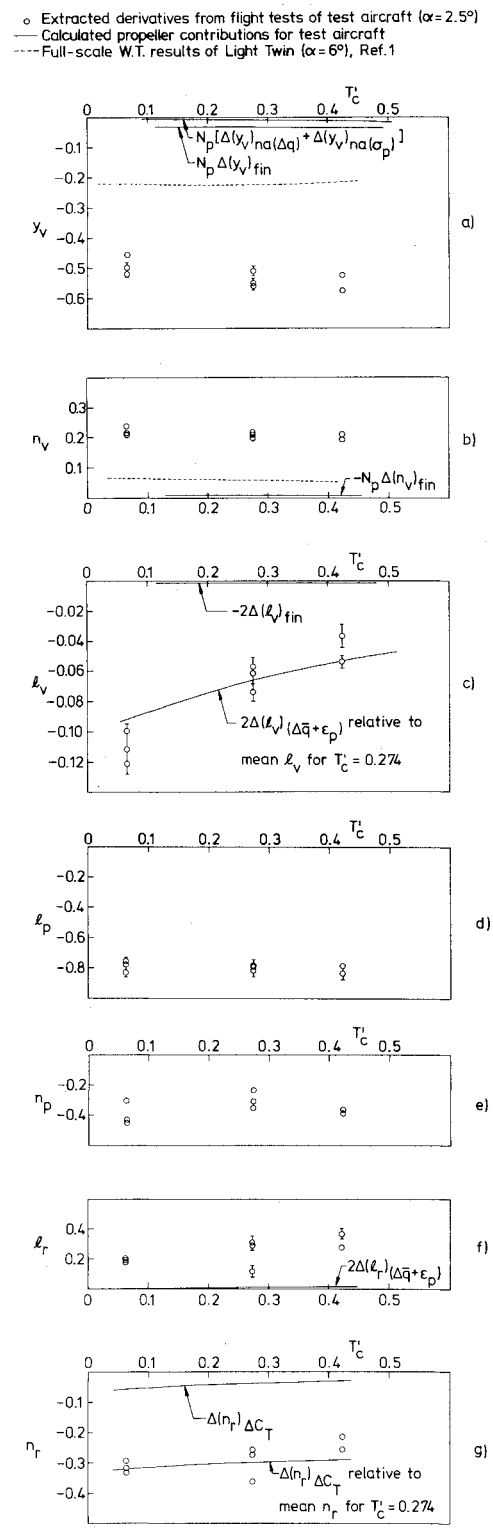

Fig. 3 Variation of stability derivatives with power (50 deg flap selected).

stream-immersed areas in sideslip:

$$\Delta(l_v)_{\text{power}} = 2 \sum_{l=i;o} [\Delta(l_v)_{(\Delta\bar{q}+\epsilon_p),l} + \Delta(l_v)_{\text{fin},l}] \tag{17}$$

where

$$\Delta(l_v)_{\text{fin},l} = -\frac{2}{b} z_{T,l} \Delta(y_v)_{\text{fin}} \tag{18}$$

The increment of lift generated at each slipstream-immersed area of the wing is a function of the increased dynamic pressure and downwash behind the propeller disks. Let $\Delta C_{L(\Delta\bar{q})}$ and $\Delta C_{L(\epsilon_p)}$ be the lift increments (per propeller) due to increased dynamic pressure and downwash, respectively, and assume these to be centered at the wing quarter chord. If it is further assumed that the lateral shift in center of pressure is equal to $x'_p \tan(\beta+\sigma_p)$ for sideslip angle β, where x'_p is the distance of the disk centers of a propeller pair from the wing quarter-chord locations of the respective immersed areas, then it can be shown[6] that:

$$\Delta(l_v)_{(\Delta\bar{q}+\epsilon_p),l} \simeq (\Delta C_{L(\Delta\bar{q}),l} + \Delta C_{L(\epsilon_p),l}) \times (x'_{p,l}/b)[1-(\partial\sigma_p/\partial\beta)] \tag{19}$$

A method to estimate $\Delta C_{L(\Delta\bar{q})}$, $\Delta C_{L(\epsilon_p)}$ is also given in Ref. 6.

The contribution $2\Delta(l_v)_{\text{fin}}$, calculated using the propeller simulation program, is shown in Fig. 3c to be negligibly small despite the large variation with T'_c at the low-speed conditions considered. The reduction in $|l_v|$ due to increasing T'_c demonstrated by the flight test results is then attributed to $\Delta(l_v)_{(\Delta\bar{q}+\epsilon_p)}$. It can be seen from Fig. 3c that for the 50 deg flap case at the incidence of concern, the low-power value of l_v is reduced to approximately half its value when full power is applied. The contribution $2\Delta(l_v)_{(\Delta\bar{q}+\epsilon_p)}$ as estimated by Eq. (19) is shown in relation to the data. To compare the predicted variation in l_v with T'_c to the variation demonstrated by the data, the estimated $\Delta(l_v)_{(\Delta\bar{q}+\epsilon_p)}$ curve is drawn relative to the mean value of the data points corresponding to T'_c for level flight. The faired flight test results for the 50 deg flap as well as a 20 deg flap case are presented with the $\Delta(l_v)_{(\Delta\bar{q}+\epsilon_p)}$ estimates in Fig. 4a and it is seen that there is fairly good agreement with the trend of the flight data.

In Fig. 4b the variation of the l_v derivative with power from full-scale wind-tunnel results of the light twin-engine aircraft of Ref. 1 is given for three flap settings. Fig. 4b was constructed by cross plotting results presented in Ref. 1, and the curves for $\Delta(l_v)_{(\Delta\bar{q}+\epsilon_p)}$ were calculated using Eq. (19). It can be seen that a similar reduction in l_v due to increasing T'_c is experienced, as obtained from flight test results. Satisfactory agreement between experimental results and estimates are thus found for both aircraft, although Eq. (19) is found to underestimate slightly for large flap deflections and to overestimate for the clean configuration. It should be noted that in Ref. 6 it is recommended that Eq. (19) be multiplied by a factor of 0.5 when used to estimate $\Delta(l_v)_{(\Delta\bar{q}+\epsilon_p)}$ for the clean configuration in lieu of comparison with data presented in Ref. 1. Some discrepancy between calculated and experimental results must be expected, since $\Delta(l_v)_{(\Delta\bar{q}+\epsilon_p)}$ is based on a relatively simple model. The two basic assumptions are that the slipstream is of uniform axial velocity and that the slipstream-immersed wing areas have definite boundaries. In practice the axial velocity is nonuniform due to a nonuniform blade loading, and the rotational velocity component of the slipstream results in the flow being spilt over these imaginary slipstream boundaries.

The extent of lateral displacement of the slipstream may also be effected by nacelle geometry, but this seems not to be the case, since the data presented are for aircraft of widely different nacelle geometries, and it is shown that Eq. (19) predicts the variation in $\Delta(l_v)_{(\Delta\bar{q}+\epsilon_p)}$ equally well in both cases.

The magnitude of the contribution $2\Delta(l_v)_{\text{fin}}$ increases with increasing speed. However, it is estimated that the upper boundary on this contribution for the test aircraft at 200 KIAS (with $\Delta(y_v)_{\text{fin}} = -0.025$) will still represent only 1% of a propeller-off wind-tunnel scale model value for l_v at the same C_L.

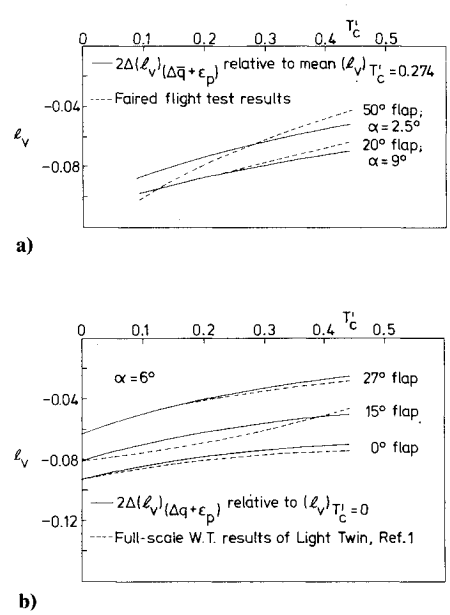

Fig. 4 Power-on effective dihedral: a) test aircraft and b) light twin-engine aircraft.

Propeller Rolling Moment due to Roll Rate

Propeller effects on l_p consist of a rolling moment due to propeller in-plane forces arising from rate of roll, and a change in damping of the wing in roll due to a change in wing lift curve slope as a result of slipstream influence:

$$\Delta(l_p)_{\text{power}} = 2 \sum_{l=i;o} [\Delta(l_p)_{(\Delta\bar{q}+\epsilon_p),l} + \Delta(l_p)_{\text{fin},l}] \tag{20}$$

where

$$\Delta(l_p)_{(\Delta\bar{q}+\epsilon_p),l} = -2[\Delta C_{L_{\alpha(\Delta q)}} + \Delta C_{L_{\alpha(\epsilon_p)}}](y_{T,l}/b)^2 \tag{21}$$

$$\Delta(l_p)_{\text{fin},l} = -4C_{Y_\alpha}(y_{T,l}/b)^2(n^2D^4/V^2S) \tag{22}$$

Estimates of the incremental changes in wing lift curve slope due to a change in slipstream dynamic pressure and downwash, respectively, are somewhat difficult to obtain; and since the extracted l_p derivatives (Fig. 3d) reflect no variation with T'_c, it is assumed that the slipstream contribution $\Delta(l_p)_{(\Delta\bar{q}+\epsilon_p)}$, which should demonstrate maximum variation at these low-speed conditions with large variations in thrust, are negligible for the test aircraft. There appears to be no other experimental data available concerning propeller influence on l_p, but in Ref. 6 estimates of $\Delta(l_p)_{(\Delta\bar{q}+\epsilon_p)}$ were made for the light twin-engine aircraft of Ref. 1 which show this contribution at high power ($T'_c = 0.44$) to be only 4% of the overall l_p estimate for an 8 deg incidence. The invariance of the l_p data over the range of thrust values presented herein suggests that the estimate of Ref. 6 is in fact of the small order indicated.

It can be shown that for the test aircraft the contribution $2\Delta(l_p)_{\text{fin}}$ is negligible at the conditions for which the data are presented, as well as at the maximum speed case which would correspond to maximum $2\Delta(l_p)_{\text{fin}}$. This was also found to be the case for the light twin-engine aircraft, Ref. 6.

Propeller Yawing Moment due to Roll Rate

Propeller effects on n_p consist of an incremental change in the wing damping in yaw due to a change in drag curve slope

as a result of slipstream influence:

$$\Delta(n_p)_{\text{power}} = 2\sum_{l=i;o}\Delta(n_p)_{(\Delta\bar{q}+\epsilon_p),l} \tag{23}$$

where

$$\Delta(n_p)_{(\Delta q+\epsilon_p),l} = 2\Delta C_{D_{\alpha(\Delta q+\epsilon_p),l}}(y_{T,l}/b)^2 \tag{24}$$

An estimate of the incremental changes in drag curve slope of the slipstream-immersed wing areas due to the increased dynamic pressure and downwash can probably be obtained only experimentally. The n_p derivatives extracted at the low-speed conditions for the 50 deg flap configuration are presented in Fig. 3e. Although there is considerable scatter of the data, the randomness of the data, as well as of data obtained for the 20 deg flap configuration, does not suggest a significant trend of n_p with the large variation in power. Therefore no attempt was made here to estimate the postulated propeller contribution $\Delta(n_p)_{(\Delta\bar{q}+\epsilon_p)}$. There appears to be no other experimental data available concerning propeller influence on n_p.

Propeller Rolling Moment due to Yaw Rate

The propeller effect on l_r is due to the rolling moment caused by the lateral displacement of the centers of pressure of the slipstream-immersed wing areas when the aircraft possesses a rate of yaw:

$$\Delta(l_r)_{\text{power}} = 2\sum_{l=i;o}\Delta(l_r)_{(\Delta\bar{q}+\epsilon_p),l} \tag{25}$$

where, from Ref. 4:

$$\Delta(l_r)_{(\Delta\bar{q}+\epsilon_p),l} = (\Delta C_{L(\Delta_q),l} + \Delta C_{L(\epsilon_p),l})(x_{p,l}/b)^2 \tag{26}$$

In Fig. 3f, $2\Delta(l_r)_{(\Delta\bar{q}+\epsilon_p)}$ as calculated from Eq. (26) is shown for the 50 deg flap case, which corresponds to a maximum possible value of this contribution, since $(\Delta C_{L(\Delta\bar{q})} + \Delta C_{L(\epsilon_p)})$ is a maximum at the largest flap deflection. It is shown that $2\Delta(l_r)_{(\Delta\bar{q}+\epsilon_p)}$ gradually increases with thrust coefficient until it represents about 8% of the mean overall l_r value at high thrust. The l_r data presented in Fig. 3f indicate a greater increase in l_r with T_c' than estimated, but it has also been found that the data obtained for a 20 deg flap selection indicate a decreasing trend with T_c'. No conclusion could be reached concerning the propeller contribution to l_r due to these conflicting results. There appears to be no other experimental data available concerning propeller influence on l_r.

Propeller Yawing Moment due to Yaw Rate

In Fig. 3g it is noted that the data for the n_r derivatives extracted at the low-speed conditions for the 50 deg flap configuration seems to suggest a power dependency despite the experimental scatter, since the derivatives corresponding to the small positive thrust value are significantly lower than n_r corresponding to full power. Possible propeller effects on n_r may be the result of 1) a contribution due to the propeller disk negative thrust gradient $\partial T/\partial V$, and 2) a change in wing contribution to n_r due to the incremental change in drag of the slipstream-immersed areas of the wing. It seems that neither of these possible effects have been dealt with in the literature before, and so they will be analyzed here.

Contribution to n_r due to $\partial T/\partial V$

Due to the lateral displacement of the propeller shafts from the c.g. of multiengine aircraft, there will be a contribution to the axial and radial inflow velocities into the propeller disks when the aircraft possesses a rate of yaw. Assuming that the propeller angular velocity $\omega \gg r$ (the rate of yaw of the aircraft), then from Fig. 5 the yaw-induced axial and radial velocity components at x on the intercept of the plane containing the propeller disk and a plane parallel to the XY aircraft plane through the center of the propeller disk are, for the case of right-hand propellers:

Port propellers: $$V_{a,p}(x) = r[(y_T - (Dx/2)]\cos i_p \tag{27}$$

$$V_{r,p}(x) = -rx_p \tag{28}$$

Starboard propellers: $$V_{a,s}(x) = -r[(y_T + (Dx/2)]\cos i_p \tag{29}$$

$$V_{r,s}(x) = -rx_p \tag{30}$$

The components of these velocities relative to a blade at azimuth θ are then (Fig. 5):

$$V_{a,p}(x,\theta) = r[y_T - (Dx/2)\sin\theta]\cos i_p \tag{31}$$

$$V_{r,p}(x,\theta) = -r[x_p - (Dx/2)\sin i_p\cos\theta] \tag{32}$$

$$V_{a,s}(x,\theta) = -r[y_T + (Dx/2)\sin\theta]\cos i_p \tag{33}$$

$$V_{r,s}(x,\theta) = -r[x_p - (Dx/2)\sin i_p\cos\theta] \tag{34}$$

The axial velocity distribution over each disk area will result in an incremental change in thrust of each propeller, due to the thrust gradient $\partial T/\partial V$, and these thrust changes will produce a yawing moment about the aircraft c.g. The resultant port and starboard thrust forces are displaced distances Δy_p and Δy_s, respectively, from the propeller shaft axes; this is due to the asymmetrical axial velocity distribution over each disk. In addition a yawing moment will also be produced due to the propeller side forces as a result of the radial velocity distribution. The total yawing moment due to the propeller pairs can therefore be written as follows in coefficient form:

$$\Delta N = \rho n^2 D^4 \sum_{l=i;o}[(y_T - \Delta y_p)C_{T_p} - (y_T + \Delta y_s)C_{T_s} + x_p(C_{Y_p} + C_{Y_s})]_l \tag{35}$$

with C_T and C_Y the integral values of the thrust and side-force coefficients, and

$$\Delta y_p = -D(C_{N_p}/C_{T_p}) \tag{36}$$

$$\Delta y_s = -D(C_{N_s}/C_{T_s}) \tag{37}$$

with C_N the integral yawing moment coefficient due to the asymmetrical thrust distribution over a propeller disk. It can be shown that to a very good approximation $C_{N_s} = C_{N_p}$ and $C_{Y_s} = C_{Y_p}$. Thus by introducing Eqs. (36) and (37) into Eq. (35), and assuming that $\Delta N \propto r$ for small perturbations in yaw, the propeller disk contribution to the derivative n_r is then given by:

$$\Delta(n_r)_{\Delta C_T} = \frac{4n^2D^5}{VSb^2r}\sum_{l=i;o}\left[\frac{y_T}{D}(C_{T_p} - C_{T_s}) + 2C_N + 2\frac{x_p}{D}C_Y\right]_l \tag{38}$$

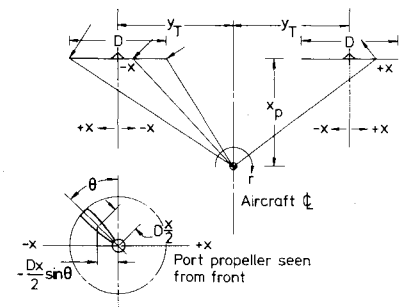

Fig. 5 Propeller inflow due to yaw rate.

Equation (38) is independent of the direction of propeller rotational velocity. The thrust differential term in Eq. (38) is the most significant of the three and it can be shown that $|\Delta(n_r)_{\Delta C_T}|$ will have maximum values at low descent speeds which would correspond to low values of thrust associated with low blade pitch settings. This is explained in more detail in Ref. 4. Since $\Delta(n_r)_{\Delta C_T}$ is negative for all conditions, the propeller disks increase the overall damping in yaw of the aircraft.

Using Eqs. (31-34) to calculate the propeller inflow, the integral thrust, sideforce, and moment coefficients were calculated by the propeller simulation computer program to obtain $\Delta(n_r)_{\Delta C_T}$ from Eq. (38) for the test flight conditions considered. In Fig. 3g $\Delta(n_r)_{\Delta C_T}$ is shown in relation to the flight data of the overall n_r derivatives extracted for three power conditions with the aircraft in a 50 deg flap configuration. The low speeds attainable at this full-flap configuration would correspond to maximum values of $\Delta(n_r)_{\Delta C_T}$ in accordance with the discussion above. It is found that $\Delta(n_r)_{\Delta C_T}$ represents 13% of the overall n_r value for the power setting corresponding to a level flight speed of 86 KIAS, and increases to 19% of this value for the small positive thrust setting. The experimental scatter of the n_r data is somewhat large, but it appears that the trend with variation in T_c' as estimated by $\Delta(n_r)_{\Delta C_T}$ is confirmed.

There appears to be only one source of experimental data concerning propeller influence on the n_r derivative, namely NACA TN 1080.[3] A value for n_r for a wind-tunnel model consisting of two pusher-type propellers mounted on a wing is presented. This configuration implies that the only propeller contribution to n_r will be $\Delta(n_r)_{\Delta C_T}$ since there is no slipstream flow over the wing. It was found that the damping in yaw was about 10% less than the damping obtained with propellers windmilling, which is to be expected in the light of the results presented above on the magnitude of $\Delta(n_r)_{\Delta C_T}$.

Contribution to n_r due to Incremental Drag Change of Slipstream-Immersed Wing Areas

Since an incremental change in axial flow velocity relative to the propeller disk results from aircraft yaw rate, it follows that there will also be a consequential change in propeller slipstream velocities which may effect the drag of the immersed wing areas. Let C_{D_i} be the propeller-off drag coefficient (induced and profile drag included) of the wing area immersed by the slipstream in the power-on condition, and let ΔC_{D_i} be the incremental change in C_{D_i} due to the slipstream, with both C_{D_i} and ΔC_{D_i} on a per-propeller basis and referenced to the total wing area. From Eqs. (31) and (33) the mean axial inflow velocity increments for one revolution of a blade of a port and starboard propeller are $ry_T\cos i_p$ and $-ry_T\cos i_p$, respectively. Assuming that the corresponding changes in slipstream velocity at the wing may be written as $fry_T\cos i_p$ and $-fry_T\cos i_p$, then the incremental change in total yawing moment from the propeller-off to the power-on condition may be written as:

$$\Delta N = \tfrac{1}{2}\rho S \sum_{l=i;o} \{ [(V - fry_T\cos i_p)^2 (C_{D_i} + \Delta C_{D_i}) y_T - (V + fry_T\cos i_p)^2 (C_{D_i} + \Delta C_{D_i}) y_T]_{\text{power on}} - [(V - ry_T\cos i_p)^2 C_{D_i} y_T - (V + ry_T\cos i_p)^2 C_{D_i} y_T]_{\text{prop off}} \}_l \quad (39)$$

Assuming that $\Delta N \propto r$ for small perturbations in yaw, then from Eq. (39) the propeller slipstream contribution to the derivative n_r is given by:

$$\Delta(n_r)_{\Delta C_D} \cong \frac{8}{b^2} \sum_{l=i;o} \{ y_T^2 [C_{D_i}(1-f) - f\Delta C_{D_i}] \cos i_p \}_l \quad (40)$$

The factor f represents the gradient of change in slipstream velocity aft of the propeller at constant blade setting, with change in the freestream inflow velocity:

$$f = \frac{\partial v}{\partial V} \quad (41)$$

The obtain an estimate for f, the propeller thrust equation $T = \rho(\pi/4)D^2(V + \tfrac{1}{2}v)v$ derived from momentum considerations is differentiated with respect to V, and the slipstream velocity v from this thrust equation is substituted into Eq. (41) to yield an expression for f in terms of thrust, thrust gradient, and velocity. After nondimensionalizing these quantities the estimate for f is given by:

$$f = \left[\frac{\partial C_T}{\partial J} + \frac{\pi J}{4} - \frac{\pi}{4}\left\{J^2 + \frac{8C_T}{\pi}\right\}^{1/2}\right] \Big/ \left[\frac{\pi}{4}\left\{J^2 + \frac{8C_T}{\pi}\right\}^{1/2}\right] \quad (42)$$

With $\partial C_T/\partial J$ negative and $[(\pi/4)\{J^2 + (8C_T/\pi)\}^{1/2} > (\pi/4)J]$, f is negative and it follows from Eq. (40) that $\Delta(n_r)_{\Delta C_D}$ constitutes a decrease in yaw damping. It can be shown that $|f|$ increases with a decrease in speed, but is less dependent on thrust variation. Using a procedure outlined in Ref. 8 to estimate ΔC_{D_i}, $\Delta(n_r)_{\Delta C_D}$ was calculated for the test aircraft at 80 KIAS with full power and 50 deg flap selected. Values of ΔC_{D_i}, C_{D_i}, and $|f|$, and thus of $\Delta(n_r)_{\Delta C_D}$, would be close to maxima at this condition, and it was found that $\Delta(n_r)_{\Delta C_D}$ represents approximately 6% of the overall n_r value extracted from flight tests.

There appears to be no other experimental data concerning propeller slipstream influence on the wing damping in yaw. Data presented in Ref. 3 for n_r of wind-tunnel model aircraft with tractor-type propellers running are not directly comparable since there may also be slipstream vertical tail interaction due to the proximity of the propeller thrust lines to aircraft centerlines.

It has been mentioned in the previous subsection that $\Delta(n_r)_{\Delta C_T}$ will be most significant at a low-speed, low-power condition; while here it was found that $\Delta(n_r)_{\Delta C_D}$ will be most significant at a low-speed, full-power condition, but is in general not sensitive to power variation at a certain speed. Thus the gain in yaw damping due to $\Delta(n_r)_{\Delta C_T}$ is reduced by $\Delta(n_r)_{\Delta C_D}$ but variation in n_r due to power variation at a certain speed will be determined by $\Delta(n_r)_{\Delta C_T}$.

Propeller Influence on Static and Dynamic Stability

Lateral and Directional Static Stability

The directional static stability is determined by n_v. It has been shown that for the low-speed condition, the destabilizing contributions $\Delta(n_v)_{\text{fin}}$ and $\Delta(n_v)_{n\alpha(\Delta\bar{q})}$ may decrease the static stability significantly, although it will not be

Table 2 Roots of the characteristic equation for three power settings

T_c'		0.066	0.274	0.422
Derivatives for	α	= 2.5 deg, 50 deg flap		
	C_L	= 1.56	1.68	1.90
	l_p	= −0.8		
	l_r	= 0.2		
	n_p	= −0.38	Invariant with power	
	n_v	= 0.2		
	y_v	= −0.54		
	l_v	= −0.11		
	n_r	= −0.32		
Small real root		−0.0326	+0.0838	+0.219
Large real root		−10.0	−9.93	−9.9
Conjugate pair of complex roots		$-1.38 \pm 6.77i$	$-1.41 \pm 6.49i$	$-1.46 \pm 6.31i$

significantly influenced by large variations in power due to the invariance of these propeller contributions with power.

The $\Delta(n_v)_{\text{fin}}$ contribution will become more important as speed is increased. However, the vertical tail contribution to n_v may also increase with increasing speed (decreasing incidence) and thus the relative importance of $\Delta(n_v)_{\text{fin}}$ to n_v will be decided by aircraft geometry, propeller location relative to the c.g. position, and propeller geometry.

Lateral and Directional Dynamic Stability

In the light of the flight test results and estimates presented, it has been noted that propeller contributions to stability may be divided roughly into two groups—the first being contributions which are significant at high- and low-speed flight conditions but do not show appreciable variation with power, for instance, $\Delta(y_v)_{\text{fin}}$ and $\Delta(n_v)_{\text{fin}}$; and the second being contributions which show significant variations with power at low-speed conditions, for instance, $\Delta(l_v)_{(\Delta\bar{q}+\epsilon_p)}$ and to a lesser extent $\Delta(n_r)_{\Delta C_T}$. Therefore it can be expected that significant changes in the lateral modes of motion due to power variation will occur at the low-speed condition, mainly as an effect of $\Delta(l_v)_{(\Delta\bar{q}+\epsilon_p)}$. This will be most pronounced for the full-flap configuration.

Using values of the derivatives for the 50 deg flap configuration presented in Figs. 3, the roots of the characteristic equation were found at three power settings, see Table 2. It has been assumed that n_v, y_v, n_p, l_p, and l_r were constant due to their demonstrated invariance with power, while the power-dependent derivatives were l_v and n_r; the variations of the latter with power were taken to be those predicted by the propeller simulation program for $\Delta(n_r)_{\Delta C_T}$.

It is noticed in Table 2 that only the small real root, which corresponds to the slow spiral motion, is significantly affected. The motion is a subsidence for the low-power value, but becomes divergent as power is increased, and the time to double amplitude for full power is only 14 s. Flight conditions corresponding to this reduced recovery time for a divergent spiral motion would be when full power is applied to climb away with full landing flap after an aborted landing, or, to a lesser extent during the takeoff climb with full power and takeoff flap deployed. Although the reduced recovery time can still be regarded as safe, the reasonably close proximity of the aircraft to the ground for both of the mentioned conditions suggests that the test for spiral stability of multiengine aircraft designs should be made for these conditions after the changes in l_v and n_r, due to $\Delta(l_v)_{(\Delta\bar{q}+\epsilon_p)}$ and $\Delta(n_r)_{\Delta C_T}$, have been accounted for. It is interesting to note that the reduction of l_v for low-speed, high-power conditions may be of importance to propfan designs now considered. A propfan would have a diameter approximately half the diameter of a turboprop producing the same thrust. Considering slipstream diameter and immersed wing area, it can be shown that $\Delta(l_v)_{(\Delta\bar{q}+\epsilon_p)} \propto 1/D$ for a given thrust, implying that the reduction in l_v due to the installed propfan would be approximately twice that for the equivalent turboprop.

The large real root, which corresponds to the roll subsidence, is not significantly affected by the changes in l_v and n_r. The real parts of the conjugate pair of complex roots, which corresponds to the damping of the dutch roll, increases slightly with power, thus increasing the already heavy damping with 50 deg flap while the frequency is slightly decreased as power is increased.

At high speed $\Delta(l_v)_{(\Delta\bar{q}+\epsilon_p)}$ and $\Delta(n_r)_{\Delta C_T}$ become insignificant and the only significant contribution is $\Delta(n_v)_{\text{fin}}$ which will reduce the dutch roll damping slightly from the assumed propeller-off value.

The only slipstream effects considered in this paper have been those influencing the wing contribution to stability. It should be noted that interaction between slipstream and horizontal tail may also occur on certain aircraft when operated at higher incidences. This interaction will result in the secondary contributions of the horizontal tail surface to l_v, l_r, and n_r being influenced to some extent, which may be estimated in a similar manner as for the wing.

The importance of wing/slipstream interaction with regard to the l_v derivative has been emphasized in this paper. It should be noted that the method of Ref. 8 which has been used here to estimate the lift increments due to slipstream from which $\Delta(l_v)_{(\Delta\bar{q}+\epsilon_p)}$ was calculated is based on an analysis by Ribner.[9] Although this method was found here to produce acceptable results, wing/slipstream interaction is treated in more recent analyses[10,11] which may provide a basis for the establishment of more rigorous analytical expressions for $\Delta(l_v)_{(\Delta\bar{q}+\epsilon_p)}$ and other slipstream-related contributions to stability cited in this paper.

Acknowledgment

This work was supported by a grant of the South African Council for Scientific and Industrial Research.

References

[1] Fink, M.P. and Freeman, D.C., "Full-scale Wind Tunnel Investigation of Static Longitudinal and Lateral Characteristics of a Light Twin-Engine Airplane," NASA TN D-4983, Jan. 1969.

[2] Fink, M.P., Shivers, J.P., and Smith, C.C., "A Wind Tunnel Investigation of Static Longitudinal and Lateral Characteristics of a Full-Scale Mockup of a Light Twin-Engine Airplane," NASA TN D-6238, April 1971.

[3] Cotter, W.E., "Summary and Analysis of Data on Damping in Yaw and Pitch for a Number of Airplane Models," NACA TN 1080, March 1946.

[4] van Rooyen, R.S., "Propeller Influence on the Lateral-Directional Stability of Multi-Engined Aircraft," Ph.D. Thesis, Cranfield Institute of Technology, Nov. 1978, Chaps. 2,5, and 6.

[5] Klein, V. and Lipscombe, M.D., "FORTRAN Program for Aircraft Parameter Estimation using the Output Error Method," Cranfield Institute of Technology, Rept. CIT-FI-76-029, Feb. 1976.

[6] Wolowicz, C.H. and Yancey, R.B., "Lateral-Directional Characteristics of Light, Twin-Engine Propeller-Driven Airplanes," NASA TN D-6946, Oct. 1972.

[7] De Young, J., "Propeller at High Incidence," *Journal of Aircraft*, Vol. 2, May-June 1965, pp. 241-250.

[8] Wolowicz, C.H. and Yancey, R.B., "Longitudinal Characteristics of Light, Twin-Engine Propeller Driven Airplanes," NASA TN D-6800, June 1972.

[9] Ribner, H.S., "Notes on the Propeller and Slipstream in Relation to Stability," NACA WR L-25, 1944.

[10] Jameson, A., "The Analysis of Propeller-Wing Flow Interaction," NASA SP-228, Oct. 1969.

[11] Butler, L., Golan L., and Miller, N., "Effects of Propeller Slipstream on V/STOL Aircraft Performance and Stability," Dynasciences Rept. DCR-137, Aug. 1974.